

A RE-EXAMINATION OF THE RELATIVE AGES OF MARE-FILLED IMPACT BASINS ON THE LUNAR NEARSIDE FROM THE GRAVITY SIGNATURES OF BURIED CRATERS. Alexander J. Evans¹, Jason M. Soderblom², Sean C. Solomon¹, and Maria T. Zuber², ¹Lamont-Doherty Earth Observatory, Columbia University, Palisades, NY 10964, USA, evans@ldeo.columbia.edu; ²Department of Earth, Atmospheric and Planetary Sciences, Massachusetts Institute of Technology, Cambridge, MA 02139, USA.

Introduction: The application of traditional crater size-frequency distribution methods [1-3] to determine the relative ages of impact basins on the lunar nearside has proven problematic because of multiple mare volcanic resurfacing events [4,5]. To estimate basin ages, previous workers have used either a patchwork of unflooded surfaces of small area [6,7] or made adjustments for mare-covered regions [6], but both of those methods introduce uncertainty and most likely bias, especially for heavily flooded basins such as Serenitatis [7,8]. More comprehensive treatments have augmented crater analyses with stratigraphic inferences to provide relative ages and sequences for lunar basins [e.g., 8], but the uncertain crater density of the pre-mare nearside surface nonetheless remains an obstacle to reliable age measurements.

Gravity data from the dual Gravity Recovery and Interior Laboratory (GRAIL) spacecraft mission [9-11] have revealed more than 100 quasi-circular mass anomalies (QCMAs), 20 km or more in diameter, beneath the nearside maria. These QCMAs are interpreted to be sites of volcanically buried impact craters [12]. In concert with previously identified surface craters [13], this population of buried craters can provide insight into the cumulative cratering rate and impact crater density of the lunar nearside.

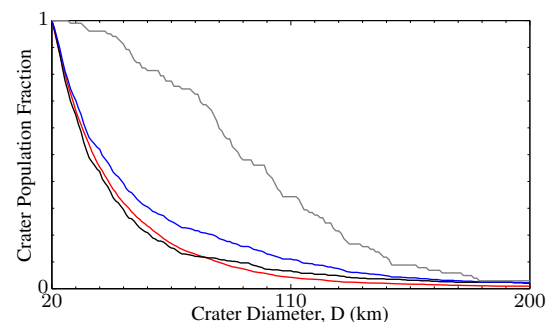
Crater Distribution: The contribution of the buried craters may be assessed with the cumulative size-frequency distribution (SFD) $N(D)$, where N is the number of craters of diameter D or greater per unit area (10^6 km²). For the buried crater population, $N(D)$ is skewed toward larger craters, with nearly half of the recovered buried craters possessing a diameter greater than 90 km (Fig. 1a). Although the techniques employed to identify QCMAs allow for recovery of long- and short-wavelength structures without amplitude bias [12], there is likely a population of smaller buried craters ($D < 90$ km) not recoverable from their gravity signatures.

There are apparent deficits of craters in nearside mare regions (see Fig. 2) compared with non-mare regions, but with the inclusion of the QCMA dataset these deficits are nearly eliminated, and mare and non-mare regions display similar cumulative SFDs for diameters $D \geq 90$ km (Figs. 1b, 2b). The nearly identical density of craters with $D \geq 90$ km in mare and non-mare regions is in contrast to the deficit of craters in the nearside maria for $D < 90$ km; this result suggests that more than half of the expected total of nearside pre-mare craters between 20

and 80 km in diameter are not recovered from gravity or topography in mare regions.

Relative Basin Ages: Given the absence of a statistically significant deficit for $N(90)$ in nearside mare regions relative to the non-mare regions (Fig. 1b), we employ $N(90)$ as a proxy for comparison of crater retention ages of lunar basins. This choice is further justified in Fig. 2, which shows maps of $N(70)$ and $N(90)$. The map for $N(70)$ shows variations that correlate with the locations of mare and non-mare regions, indicating that at $D = 70$ km the burial of pre-mare craters has not been fully corrected. Overall, we find general consistency with the relative ages given by Wilhelms [8] (Table 1), with the notable exception of Crisium.

(a)



(b)

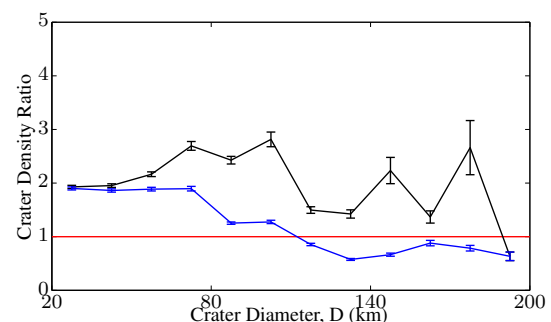


Figure 1. Distribution of craters by diameter ($D \geq 20$ km). **(a)** Crater population fraction, defined as $A \times N(D) / N(20)$, where A is the counting area. Crater populations shown represent non-mare regions (red), buried craters (gray), mare regions (black), and mare regions with buried craters included (blue). **(b)** Frequency ratio of craters in non-mare regions to mare regions shown with (blue) and without (black) buried craters. Solid lines give the ratio of incremental SFDs for a 15-km bin size in diameter, and error bars follow from the standard error in the individual SFDs derived from variations over areas equal to a square degree at the equator. The red line denotes a 1:1 ratio.

Serenitatis. Although generally mapped as Nectarian in age, *Serenitatis* lacks nearly half the craters more than 90 km in diameter needed to have a crater SFD consistent with those of such other Nectarian impact basins as *Nectaris*, *Humboldtianum*, and *Humorum* (Table 1). Instead, *Serenitatis* has an $N(90)$ value indistinguishable from that of *Imbrium*, consistent with the interpretation by Wilhelms [8] of a relatively young age for this basin.

Crisium. Cumulative crater SFDs for *Crisium* have consistently indicated a deficit of large craters ($D \geq 90$ km) [6,7,13] for a basin of its inferred stratigraphic age. Although such a deficit could previously have been attributed to burial by mare deposits, our study reveals that *Crisium* is deficient by more than 50% of the expected number of large craters relative to other basins of similar stratigraphic age. Thus, either *Crisium* is younger than *Imbrium* and *Serenitatis* and nearly as young as *Orientalis*, or it must have experienced a crater removal process subsequent to the *Serenitatis* and *Imbrium* impacts. Such removal cannot have been through viscous relaxation, because that process preferentially affects longer wavelengths and such a pattern is not evident in the overall topographic or gravitational structure of the basin. If the pre-impact topography and crust were similar in elevation and thickness, respectively, to those of the surrounding region, a high-energy, asymmetric impact could account for extensive excavation [14], lack of *Serenitatis* ejecta, and deficit of large craters, but only if that impact postdated *Imbrium*. An asymmetric ejecta distribution could also account for the lack of observed *Crisium* ejecta in *Serenitatis* and the identification of *Imbrium* ejecta north of Mare *Crisium* [8].

Summary: Although the record of pre-mare impact craters has been modified by mare volcanism for crater diameters as large as 100 km, for diameters greater than 90 km that record is well preserved in the lunar gravity field. The buried craters may not be identifiable in surface morphology or altimetry, but their inclusion yields a nearside crater population that provides a useful proxy to assess the preservation age and chronology of the pre-mare lunar surface. With the exception of *Crisium*, which has an anomalously young crater retention age, the relative ages of large basins are in general agreement with the nearside basin chronology of Wilhelms [8].

References: [1] Neukum, G., et al. (1975), *Moon*, 12, 201–229. [2] Neukum, G., and B. A. Ivanov (1994), in *Hazards due to Comets and Asteroids*, ed. by T. Gehrels, Univ. Arizona Press, pp. 359–416. [3] Le Feuvre, M., and M. A. Wieczorek (2011), *Icarus*, 214, 1–20. [4] Head, J. W. (1976), *Rev. Geophys. Space Phys.*, 14, 265–300. [5] Solomon, S. C., and J. W. Head (1980), *Rev. Geophys. Space Phys.*, 18, 107–141. [6] Hartmann, W. K., and C. A. Wood (1971), *Moon*, 3, 1–78. [7] Fassett, C. I., et al. (2012), *JGR*, 117, E00H06. [8] Wilhelms, D. E. (1987), *The Geologic History of the Moon*, U.S. Geol.

Survey Prof. Paper 1348. [9] Konopliv, A. S., et al. (2013), *JGR Planets*, 118, 1415–1434. [10] Lemoine, F. G. et al. (2013), *JGR Planets*, 118, 1676–1698. [11] Zuber, M. T. et al. (2013), *Science*, 339, 668–671. [12] Evans, A. J. et al., (2013), *AGU Fall Meeting*, abstract G31B-05. [13] Head, J. W. et al. (2010), *Science*, 329, 1504–1507. [14] Wieczorek, M. A. et al. (2013), *Science*, 339, 671–675. [15] C. I. Fassett and J. W. Head (2008), *Icarus*, 195, 61–89.

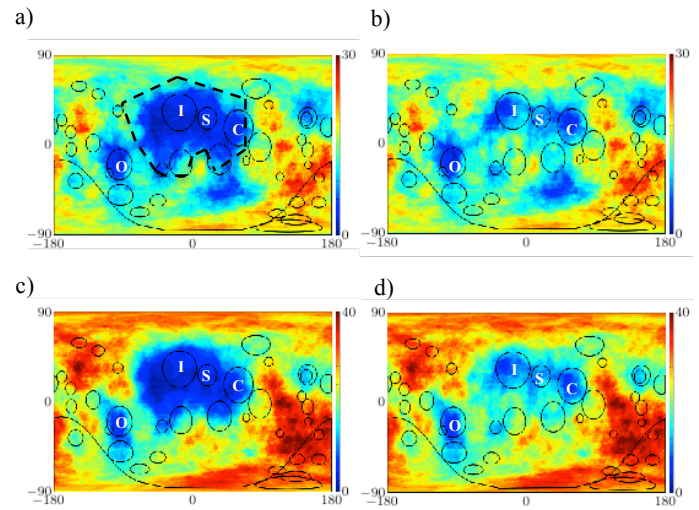


Figure 2. Map of $N(D)$ (averaged over a circular window of 500-km radius). (a and b) $N(90)$ with and without QCMA, respectively. (c and d) $N(70)$ with and without QCMA, respectively. The thick dashed line in (a) outlines the mare regions as adopted for this study. Basins with diameters larger than 250 km are outlined in black. The Imbrium (I), Serenitatis (S), Crisium (C), and Orientale (O) basins are identified.

Basin	Period	$N(20)$	$N(90)$		
			Total	QCMA	QCMA (%)
South Pole-Aitken	PN	156±7	18.8	-	-
Nubium	PN	195±18	23.7	7.3	31
Smythii	PN	225±19	17.8	-	-
Nectaris	N	135±14	13.7	6.1	44
Humboldtianum	N	93±14	14.0	-	-
Humorum	N	108±21	15.3	0.0	0
Crisium	N	113±11	4.3	1.1	25
Serenitatis	N	298±60	8.8	2.9	33
Imbrium	I	30±5	9.2	6.2	67
Orientalis	I	21±4	3.0	-	-

Table 1. Cumulative SFD, $N(D)$, for selected basins, listed in order of decreasing inferred stratigraphic age [8]. Periods are Pre-Nectarian (PN), Nectarian (N), and Imbrian (I) [8]. $N(20)$ values are from Fassett et al. [7]. For $N(90)$, “Total” represents $N(D)$ with the QCMA population included, “QCMA” represents $N(D)$ for the QCMA population only, and “QCMA (%)” is the cumulative SFD for QCMA as a percentage of the total SFD. A dash symbol for the QCMA column indicates that the basin was not examined for QCMA. $N(D)$ was determined from craters interior to or superposed on the rim of the basin [15]. The standard error for $N(90)$ is less than 2.